Induced-drag reduction of wing–wings and wings–ground configurations

L. Marino
Department of Mechanics and Aeronautics
University of Rome
Italy

ABSTRACT

The problem of induced drag reduction during formation flight is revisited by means of a simple aerodynamic model based on lifting line theory. The optimum configuration for minimum induced drag is analysed both in and out of the ground effect and the influence of the main geometrical and aerodynamic parameters is considered. The results are discussed and compared with existing numerical and experimental data.

NOMENCLATURE

A	surface area
AR	aspect ratio
b	wing span
c	wing chord
C_D	induced drag coefficient
C_l	sectional lift coefficient
C_L	lift coefficient
f	constraint function
F	objective function
h	altitude
Ma	Mach number
s	vortex semiwidth
S	surface
V	velocity
w	downwash
W	weight
x,y,z	Cartesian co-ordinates
X	independent variables in the optimum problem
α	angle-of-attack
Γ	vortex strength
φ	wing twist angle
Δx	streamwise relative distance
Δy	spanwise relative distance
Δz	vertical relative distance
λ	wing taper ratio

Subscripts

r	wing root
t	wing tip
s	single wing
∞	free stream flow condition

1.0 INTRODUCTION

The reduction of drag is a challenging and important issue for both applied and theoretical fluid-dynamicists. In particular, the reduction of the induced component of aircraft drag has been investigated ever since the first fixed-wing aircraft first flew and several solutions have since been proposed and studied. Among the various

Paper No. 2883. Manuscript received 5 March 2004, revised version received 10 May 2004, accepted 1 June 2004.

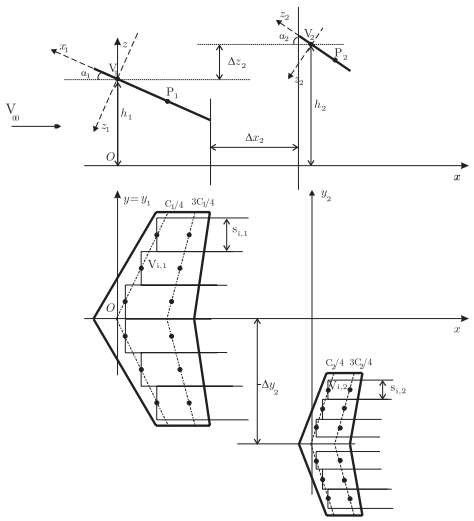

Figure 1. Sketch of the model for two wings.

possibilities, suitable formation flight of a group of aircraft and/or flight in presence of ground effect have been considered as a way to obtain a sensible improvement in terms of induced drag reduction. Both these options are investigated in the present paper which, in particular, concerns questions such as to the minimum induced drag of a single aircraft and of a formation in ground effect, and the ground effect on wings at negative angles-of-attack. The analysis is particularly aimed at a better comprehension of the influence and effectiveness of the aerodynamic and geometric parameters which characterise the problem.

The paper begins with a short review of the pertinent literature on the topic, including the main numerical and experimental contributions. A description of the adopted methodology is then reported, stressing the original contribution here introduced and including a comparison against already published results in a specific section. The paper concludes with a final discussion of the main results of the present work.

Interest in formation flight was mainly devoted in the past to the analysis of induced drag reduction which follows suitable configurations of the formation. It is usual to refer to the flight of migrating birds which are often observed to obtain benefit flying in formation and a number of papers cover this particular subject[1-4]. Suffice to recall that Hainsworth[2,3] observed Canadian geese and brown pelicans flying in formation, the latter also in ground effect. His considerations were based on the analysis of recorded films, and concerned statistics of the most frequent geometrical configurations. Neither aerodynamic models, nor quantitative results were given in those papers while Hummel[4] applied a simple aerodynamical model to the formations of birds and reported on the main characteristics concerning wing-twist, roll control and weight distributions.

Turning now to the flight of aircraft we note that progress in induced drag reduction is strictly dependent on experience, experiments and – from a speculative point of view – upon progress in computational simulations. The fundamental ideas underlying methods for induced drag prediction and reduction were reviewed by Kroo in Ref. 5 In particular, in recent times more and more accurate numerical solutions of the incompressible aerodynamic field around the entire aircraft have been obtained as more and more powerful computer codes have been made available; beginning with the Boundary Elements Method, in the inviscid case with its boundary layer corrections, and ending with the solvers of the Reynolds averaged Navier-Stokes equations. The range of application and the accuracy of those numerical procedures have been improved and promoted by the computers power and by their price evolution. Despite this progress there are still situations, like those dealt with in this work, where a fast and simple although less accurate answer is sought, and the use of sophisticated numerical programs is unnecessarily time consuming, expensive and, in some cases at least, unreasonable if not impossible. As a significant example, we just cite the problem where a number of combinations of lifting and non-lifting surfaces fly in formation and are, possibly, in ground effect.

The problem of optimal formation of aircraft in flight has been previously addressed by means of simplified aerodynamic models[6-8]. Iglesias and Mason[6] calculated the optimum span load distributions to achieve the minimum induced drag of a group of three equal wings in symmetric V formation flight. As pointed out in that paper, the load distributions were evaluated with the constraints of constant lift and a trimmed roll moment and as a result of an optimisation procedure where the actual shape of the wing was not taken into account but only the vorticity distributions were calculated. The effects of the streamwise, spanwise and vertical distances are presented[6] in terms of the relative changes with respect to the optimal value (corresponding to an elliptic load distribution) for an isolated wing.

A mixed horseshoe-vortex and vortex-lattice approach has been used by Bloy and Trochalidis Ref. 8 to calculate the aerodynamic coefficients of a tanker-receiver system which has been also experimentally studied in a wind tunnel. Although that paper addressed the receiver's behaviour in terms of pitching and rolling moment coefficients in the wake of the tanker, the simple numerical approach gave a good example of a methodology to investigate the overall drag of the formation.

In the following we will revisit a model which appeared in a couple of rather old reports[9,10] and was proposed for the vortical representation of a system of lifting and non lifting surfaces in an inviscid and incompressible flow.

That model, which will be adopted and extended in this paper, is based on the lifting line theory, as fully described in[11-12], and was chosen for its solution methodology of the basic aerodynamics of wings, inclusive of the rapid estimation of the spanwise load distribution[13]. We extended the capabilities of the model by giving it a more general form than the original one to make it suitable not only for computations of the aerodynamic coefficients of a single wing, but also for evaluating the flow field around aerodynamically interacting systems of surfaces. This means that, apart from the calculation of the lift, induced drag and moment coefficients of each wing, the distribution of the velocity components and of the pressure can be computed and represented in the entire three dimensional space around the surfaces.

The map of the velocity field gives a further tool to understand the physical reasons for reduction of drag when formation flight and/or ground effect are taken into account. With regard to this point, some conclusions at the end of the paper are also based on the analysis of the distributions of velocity and pressure, although they are not reported here for the sake of brevity.

In all cases, the generalised aerodynamic model was made reliable and efficient for solving the problem of optimising the flight formation. When wings in formation are treated, the main requirement is to keep the lift force of each wing constant. In so doing and for all problems to be discussed, it is assumed that pitch equilibrium is also satisfied.

2.0 THE MODEL

To fix the geometry of the problem we refer to Fig. 1 where a formation of two wings is represented. More generally, each one of a system of J surfaces $S_j (j = 1,..J)$ corresponds to a set of N rectangular horseshoe vortices of strength $\Gamma_{i,j}$ $(i = 1,..,N)$ which are placed along the quarter-chord lines.

As a straightforward application of the Biot-Savart law, the induced velocity is calculated in any point of the three-dimensional domain around the vortex system. The boundary condition of impermeability on the resultant flow is imposed at the three-quarter chord

https://doi.org/10.1017/S000192400000035X Published online by Cambridge University Press

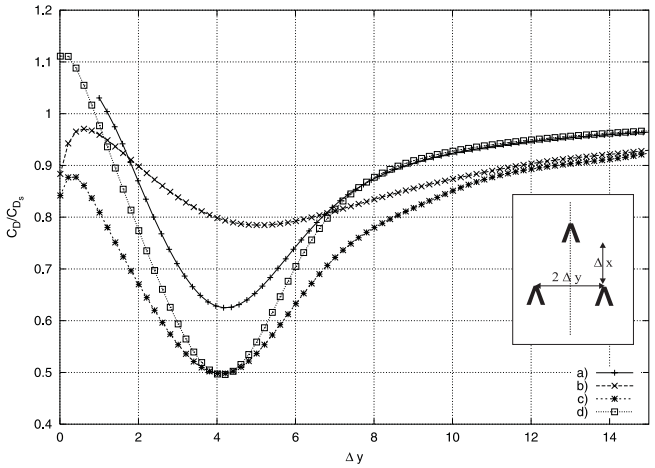

Figure 2. $C_D/C_{D,s}$ of each of the two trailing wings as a function of Δy, for $\Delta z = 0$.
a) $\Delta x = 3$, $\alpha_1 = 5°$; b) $\Delta x = 30$, $\alpha_1 = 5°$;
c) $\Delta x = 30$, $\alpha_1 = 1°$; d) $\Delta x = 3$, $\alpha_1 = 1°$.

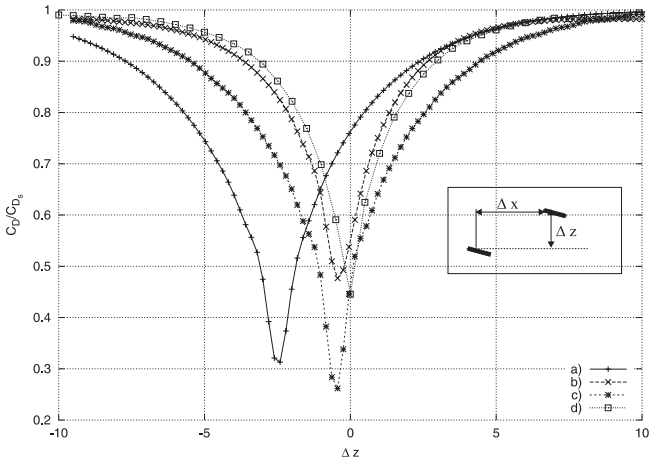

Figure 3 . $C_D/C_{D,s}$ of each of the two trailing wings as a function of Δz, for $\Delta y = 5$.
a) $\Delta x = 3$, $\alpha_1 = 5°$; b) $\Delta x = 30$, $\alpha_1 = 5°$;
c) $\Delta x = 30$, $\alpha_1 = 1°$; d) $\Delta x = 3$, $\alpha_1 = 1°$.

line of each S_j[14]. The application of this condition gives a set of $N \times J$ algebraic equations for the unknown circulation strengths $\Gamma_{i,j}$ of each horseshoe vortex.

We remark that we put no limitations on the specific type of surface S_j, which can represent an aircraft wing as well as a fixed or a mobile surface (flap, aileron, stabiliser, elevator, fin) or appendices (engine pylon, end plate, winglet).

The span loading distribution is obtained by means of the Kutta-Joukowsky relationship, and the induced drag of each wing is calculated via the evaluation of the induced downwash. Here we report only that part of the theory which is related to the computation of the aerodynamic coefficients, the complete expressions for the induced velocity are reported in Appendix A.

The solution of the algebraic system, which governs the unknown strengths of the vortices, provides $\Gamma_{i,j}$ in the vector form ($\Gamma_{1,1}$,..., $\Gamma_{N\times J}$). The lift coefficient $C_{L,j}$of S_j and the corresponding span loading coefficient $(C_l c)_{i,j}$ at a point $V_{i,J}$ are then obtained from;

$$C_{L,j} = \frac{4}{(V_\infty A_j)} \sum_i \Gamma_{i,j}\, 2s_{i,j} \qquad \ldots(1)$$

$$(C_l c / C_L c_{av})_{i,j} = \frac{b_j \Gamma_{i,j}}{\Sigma_i \Gamma_{i,j} s_{i,j}} \qquad \ldots(2)$$

where A_j is the area of the j-th wing, $s_{i,j}$ is the semiwidth of the i-th vortex on it, b_j is the j-th wing span and $c_{j,av}$ is the j-th average chord. The assigned geometrical properties of each surface, such as taper ratio $\lambda = c_t/c_r$, aspect ratio $AR = b^2/A$, sweep angle Λ, twist angle φ, are obtained by a proper distribution of the vortices and the angle-of-attack. Following the lifting-line theory, the induced drag coefficient is then calculated as;

$$C_{D,j} = -\frac{4}{(V_\infty A_j)} \sum \Gamma_{i,j}\, w_{i,j}\, 2s_{i,j} \qquad \ldots(3)$$

with $w_{i,j}$ the downwash at $V_{i,j}$.

The presence of the ground or, in general, a wall is taken into account by the reflected image representation of each S_j .

The algorithm convergence was successfully tested and numerical errors of the order of 10^{-4} or lower, for the lift and drag coefficients were obtained when $N = 120$ vortices were located on each surface.

Turning now to the optimisation procedure, in our computational code we evaluated the minimum induced drag either of each single wing in the formation or of the group of wings as a whole. The optimisation algorithm minimises a non-linear objective function $F = F(X)$ subject to the constraint functions $f_l(X)$, $l = 1,..,L$. The constraints include simple bounds on the independent variables X_m, $m = 1,..,M$ (distances between the wings, geometrical characteristics of the surfaces, etc.), and other linear or non-linear constraints (e.g. an assigned value of the lift coefficient C_L of each wing). After optimisation, the set X_m gives the optimal configuration for the objective function F chosen. The numerical procedure is based on a sequential quadratic programming method[15] where the Jacobian matrix is expressed in terms of finite differences.

With reference to Fig. 1, a Cartesian system of co-ordinates has its origin in the middle of the vortex representative of the first wing and the configuration of the formation is described by the relative distances Δx_j, Δy_j, Δz_j, made dimensionless with respect to the chord at the wing root of the first aircraft. Here:

- Δx_j is the distance along x between the trace, on the symmetry plane, of the trailing edge of the preceding wing $S_j - 1$, and the trace, on the symmetry plane, of the leading edge of the wing S_j which follows.
- Δy_j is the distance, in y-direction, of the planes of symmetry of the wings S_1 and S_j.
- Δz_j is the distance along z between the one quarter chord points in the symmetry planes of S_1 and S_j.

As a final remark, note that no attempt has been made to deal with longitudinal equilibrium and trimming. The constraint of a constant value of the lift for each and all aircraft has been imposed by properly changing the angles-of-attack of the trailing aircraft, with respect to the leading one.

3.0 RESULTS

The presentation of results begins with a few comparisons with already existing numerical and experimental data. For the sake of clarity, in each picture a little sketch of the configuration investigated is reported. A flipped heavy Λ symbol was chosen to represent an aircraft in the horizontal plane $x - y$ while a small heavy dash has been adopted in the vertical plane $x - z$.

When we make a first comparison of our results with those in[6], we note the intrinsic differences between two approaches. In our case the complete geometric characteristics of the wings are assigned (planform shape and wing twist and chord camber

https://doi.org/10.1017/S000192400000035X Published online by Cambridge University Press

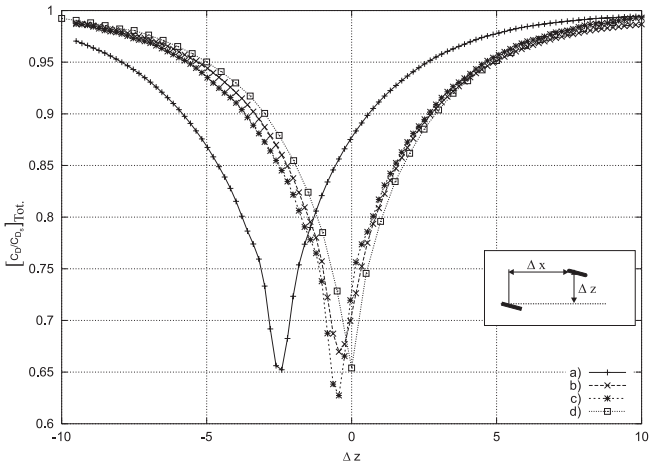

Figure 4. $[C_D/C_{D,s}]_{Tot}$ of a formation of three wings as a function of Δz, for $\Delta y = 5$.
a) $\Delta x = 3$, $\alpha_1 = 5°$; b) $\Delta x = 30$, $\alpha_1 = 5°$;
c) $\Delta x = 30$, $\alpha_1 = 1°$; d) $\Delta x = 3$, $\alpha_1 = 1°$.

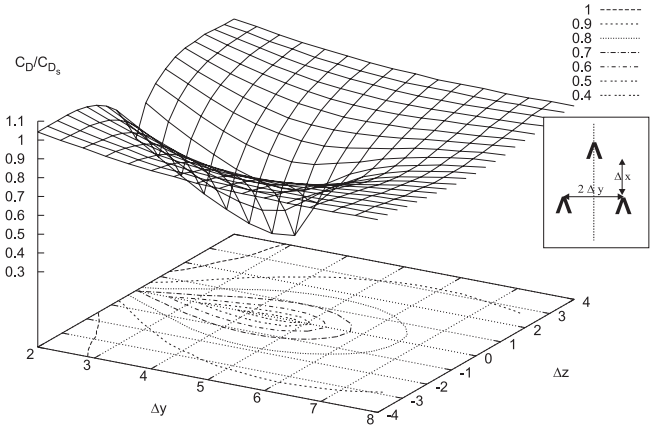

Figure 5 . Distribution and contour plots of $C_D/C_{D,s}$ of each of the two trailing wings for $\Delta x = 3$, $\alpha_1 = 1°$.

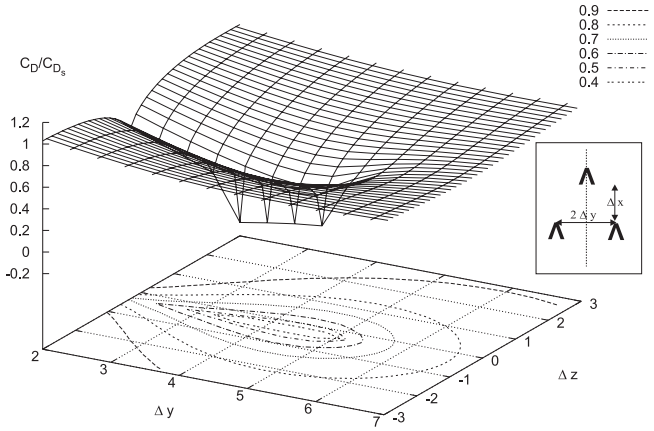

Figure 6 . Distribution and contour plots of $C_D/C_{D,s}$ of each of the two trailing wings for $\Delta x = 3$, $\alpha_1 = 5°$.

Table 1
Optimal values of Δz_{opt} and $(C_D/C_{D,s})_{min}$ of each of the two trailing wings, for $\Delta y = 5$

α_1(deg)	Δx	Δz_{opt}	$[C_D/C_{D,s}]_{min}$
5	30	–2·41	0·27
5	3	–0·32	0·45
1	30	–0·48	0·27
1	3	–0	0·40

distributions) whereas in Ref. 6 only the planform geometry is given and, as we said, the loads and downwash angles are calculated from the minimum induced drag requirement. However, a similar behaviour of the induced drag variations – by the two procedures – can be demonstrated. Our results are shown in Figs 2-6. The induced drag C_D is referred to the value $C_{D,s}$ of a single wing under the same freestream conditions and at the same value of the lift coefficient C_L.

Figures 2–6 show the effect of the spanwise Δy and vertical Δz separations for a group of three equal, rectangular, untwisted wings of aspect ratio AR = 10, at fixed values of the lift coefficient and streamwise distance x. In particular, Figs 2 and 3 present $C_D/C_{D,s}$ of the trailing wings for two values of the angle-of-attack α_1 and of Δx.

No subscripts are used for the distances between the leading and the two trailing wings, as there is no ambiguity in this particular symmetrical configuration.

We note that the reduction of the induced drag of the trailing wing depends on the strengths and spatial distributions of the vortices of the leading wing, which are directly related to the lift and which change with the angle-of-attack of the wing itself. The different spatial structures of the vortices after the leading wing are responsible for the different vertical separations Δz to achieve the minimum $C_D/C_{D,s}$. The data in Fig. 4 are particularly significant as they show that the maximum reduction of the induced drag of the entire formation $[C_D/C_{D,s}]_{min}$ does not change too much, when the parameters α_1 and Δx are changed, although the configuration (Δz) to obtain this benefit changes. This fact confirms Munk's theorem[16].

The results of the optimisation procedure for $\Delta y = 5$ are summarised in Table 1 where the optimum values $\Delta z = \Delta z_{opt}$ and the corresponding $[C_D/C_{D,s}]_{min}$ are shown for different x. The smoothing of the data in Fig. 3 introduces a little graphical error with respect to the exact values of the Table.

A spatial representation of the influence of Δz and Δy on $C_D/C_{D,s}$ for two values of the angle-of-attack α_1, is shown in Figs 5 and 6, where the corresponding contour levels are also given

Since the present calculations are based on a wing theory which is – in principle – valid for intermediate and great AR values, we made a test in order to evaluate its lower acceptable limits. Thus we run our code in the case of a low-aspect ratio delta wing ($AR = 2$) and compared the results in Fig. 7 with those obtained by Polhamus theory[17] and with the experimental data[18].

We recall that in Ref. 17 the lift is made of two parts, the first one corresponding to a plane vortex sheet adjacent to the wing and the second associated to two vortices detaching from the leading-edges. The second term plays a relevent role only at great α.

After carrying out this test with good results, provided that α is relatively small, we felt confident to deal with a less extreme case and we considered the formation of two F/A-18s as in the experimental flight test in Ref 19.

The simulated trapezoidal wings have now a wing span b = 11·34m, a root and tip chord c_r = 4·04m and c_t = 1·68m , respectively, and a surface area A = 37·16m^2. Correspondingly the aspect ratio is AR = 3·5, the taper ratio λ = 0·416 and the sweep back angle at the quarter-chord line $\Lambda_{0.25} = 20°$.

Taking into account the flight conditions at a Mach number Ma = 0·56, at an altitude h = 25,000ft and for a weight W = 18,000kg, the

https://doi.org/10.1017/S000192400000035X Published online by Cambridge University Press

lift coefficient was assumed $C_L = 0{\cdot}58$. The results shown in Fig. 8 are to be compared with analogous data of Ref. 19 where a streamwise separation $\Delta x = 3b$ was considered. The contour levels of the induced drag variations are shown, as functions of y and z, and a good agreement is found with respect to the experimental results. The circle-like curve with label A in Fig. 8, partially reports the data in Ref. 19 and corresponds to $[C_D/C_{D,s}]_{Tot} = 0{\cdot}4$. In particular, reasonable agreement is recognised in terms of the location of the optimal wings, while a rather appreciable difference is found in the C_D values. This last point is firstly explained by the assumption of constant weight W (and, consequently, C_L) adopted in our analysis, whereas the flight-measured drag reduction takes into account a quite rapidly fuel consumption. Furthermore the geometrical data relative to the specific F-18 aircraft of the experiments could be only approximatively known by the author.

At this point, our analysis proceeds with the investigation of a number of aircraft larger than the ones assumed for comparisons with existing data. When a group of five identical wings (with the same geometrical characteristics of the ones reported in Figs 2-6) is considered for a symmetrical V-configuration, the increased number of degrees of freedom, in terms of the relative distances, gives a richer panorama for the possible distributions of $C_D/C_{D,s}$. In particular all the distances , Δx_1, Δy_1, Δz_1, and x_2 , y_2, z_2 can be arbitrarily chosen.

Figures 9 and10 show the total $[C_D/C_{D,s}]_{Tot}$ of the formation for different values of Δy_1 and Δy_2, and a different and more complex scenario is immediately seen when compared with the simpler case of three wings (i.e. Fig. 2). Two configurations corresponding to a local minimum for the total induced drag $[C_D/C_{D,s}]_{Tot}$ can be observed. Such a result is also recognised in Fig. 10, for the cases *b), c) and d*), which reports the distributions of $[C_D/C_{D,s}]_{Tot}$ for four values of Δy_1. These results are to be evaluated not only from the point of view of aerodynamics, but also taking into account other constraints, as, for example, those concerning flight control, which can reduce the overall benefit of drag reduction.

When the presence of the ground is considered, further drag reduction can be obtained when flying in formation. The ground effect has been deeply investigated in the case of a single aircraft[21,22] and is still considered for new possible commercial applications[22].

In the last part of this paper the combined effects of both the ground presence and the formation flight are considered.

Figure 11 shows the influence of decreasing the altitude of three untwisted rectangular wings with AR = 10, on the induced drag of a - *V* - flight formation. The altitude was made dimensionless with respect to the root chord of the first wing. This formation already appears in Fig. 4 where, for $h \Rightarrow \infty$, one has $[C_D/C_{D,s}]_{\mathrm{Tot}} = 0{\cdot}87$. The further noticeable drag reduction due to the ground, also at an altitude of about 10 chords, can be explained by observing that the wake of the leader, at a sufficiently great distance as $\Delta x = 30$, has been significantly distorted by the presence of the ground. This reduction of the downwash is the cause for the associate reduction of C_D .

Figure 12 reports the induced drag for a formation and should be compared with Fig. 13 where the analogous case is studied out of ground effect. Figures 14 and 15 show the results of the total induced drag for a number of flight configurations at different altitudes. The benefits of the ground proximity are evident. Note that the optimal values are obtained for fixed Δy, Δx and α_1 at practically equal values of the vertical displacement Δz, no matter what the value of the altitude.

The presence of the ground at very low h, as modelled by the present theory, is cause of a sizeable decrease of the total induced drag not only in optimal conditions but also when the trailing wing flies at large negative values of Δz. In these last conditions a strong nonlinear interaction of the vortical system of the three wings is felt.

As a final result the problem of a single wing at a negative angle-of-attack is shown in Fig. 16. This case is usually of interest for race car applications. The experimental results of Ref. 23 and those

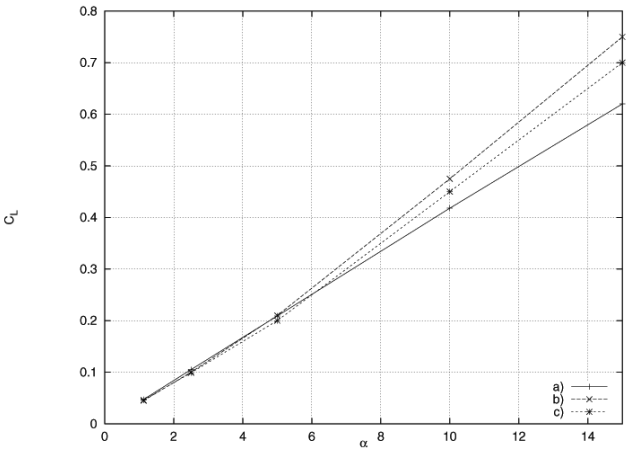

Figure 7. Lift coefficient *vs* the angle-of-attack α for a delta wing with $AR = 2$.
a) Present calculation.
b) Polhamus theory[17]
c) Experimental results[18].

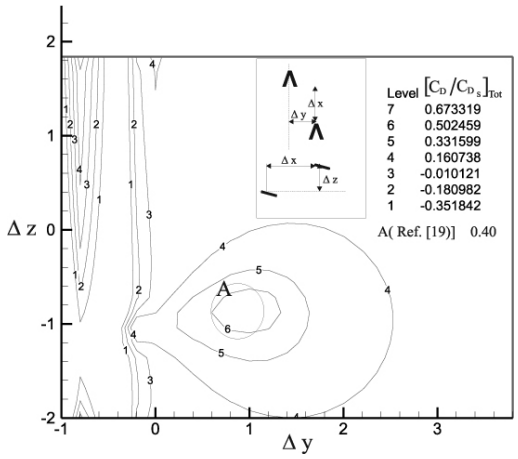

Figure 8. Induced drag reduction $[C_D/C_{D,s}]_{Tot}$ for a formation a two F 18/A aircraft. Same configuration as the one reported in Ref. 19.

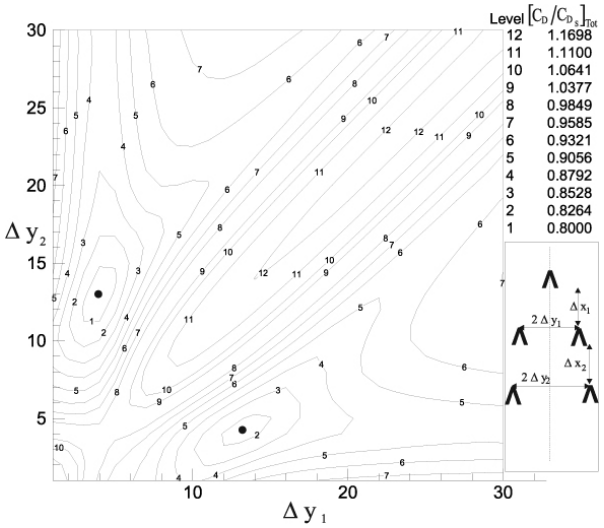

Figure 9. Contour plots $[C_D/C_{D,s}]_{Tot}$ of the formation of five wings as a function of Δ_{y_1} and Δ_{y_2}. $\alpha_1 = 5°$, $\Delta_{x_1} = \Delta_{x_2}$=10, $\Delta_{z_1} = \Delta_{z_2} = 0$.

https://doi.org/10.1017/S000192400000035X Published online by Cambridge University Press

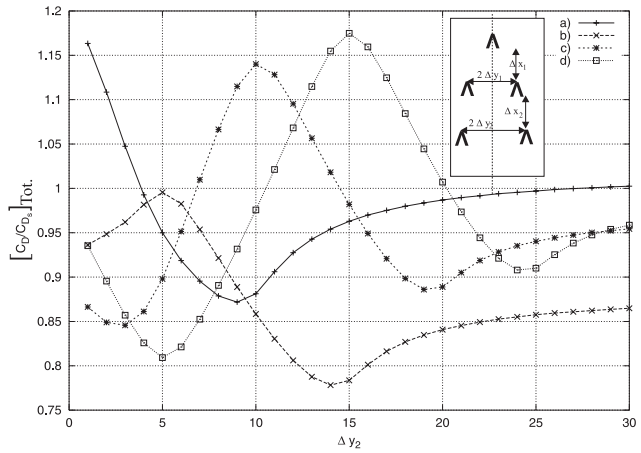

Figure 10. Contour plots $[C_D/C_{D,s}]_{Tot}$ of the formation of five wings as a function of Δ_{y_2}, for $\alpha_1 = 5°$, $\Delta_{x_1} = \Delta_{x_2} = 10$, $\Delta_{z_1} = \Delta_{z_2} = 0$.
a) $\Delta_{y_1} = 0{\cdot}1$; b) $\Delta_{y_1} = 5$; c) $\Delta_{y_1} = 10$; d) $\Delta_{y_1} = 15$.

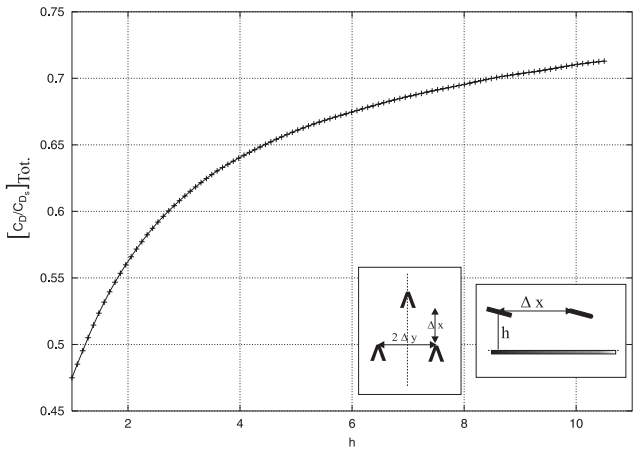

Figure 11. Total induced drag of a formation of three wings in ground effect *vs h*.
$\Delta z = 0$, $\Delta y = 5$, $\Delta x = 30$, $\alpha_1 = 5°$.

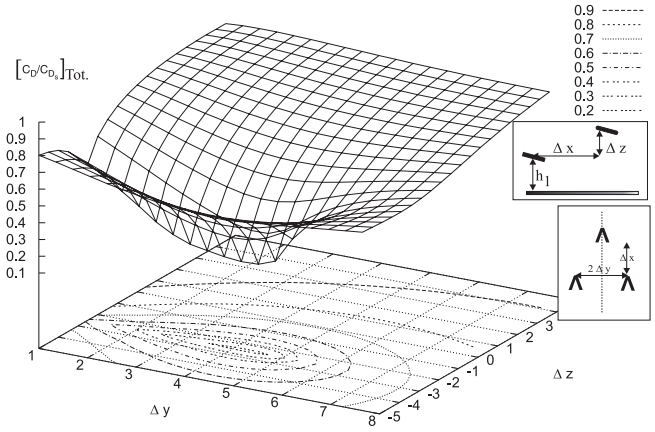

Figure 12. Total induced drag $[C_D/C_{D,s}]_{Tot}$ for a formation of three wings in ground effect *vs* Δz, Δy.
$\Delta x = 30$, $h_1 = 10$, $\alpha_1 = 5°$.

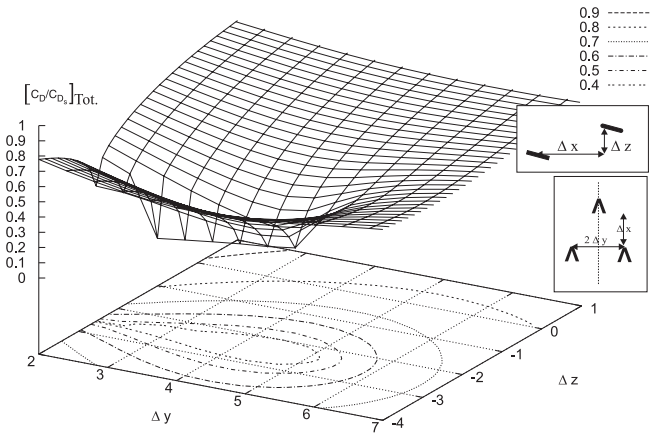

Figure 13. Total induced drag $[C_D/C_{D,s}]_{Tot}$ for a formation of three wings out of ground effect *vs* Δz, Δy.
$\Delta x = 30$, $h_1 = \infty$, $\alpha_1 = 5°$.

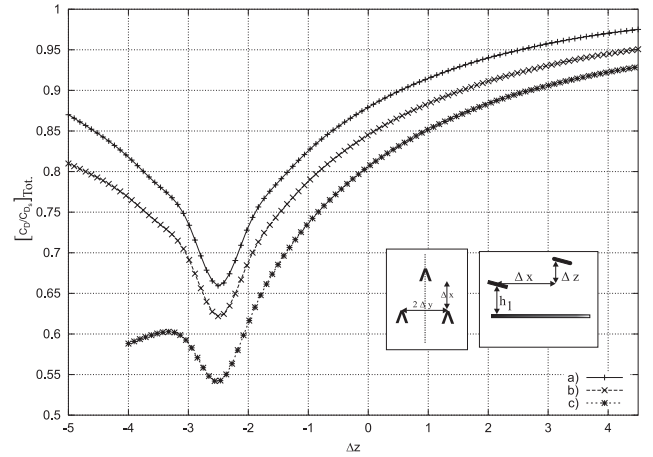

Figure 14. Total induced drag $[C_D/C_{D,s}]_{Tot}$ for a formation of three wings in ground effect *vs* Δz,
$\Delta y = 5$, $\Delta x = 30$, $\alpha_1 = 5°$.
a) $h_1 = \infty$; b) $h_1 = 10$; c) $h_1 = 5$.

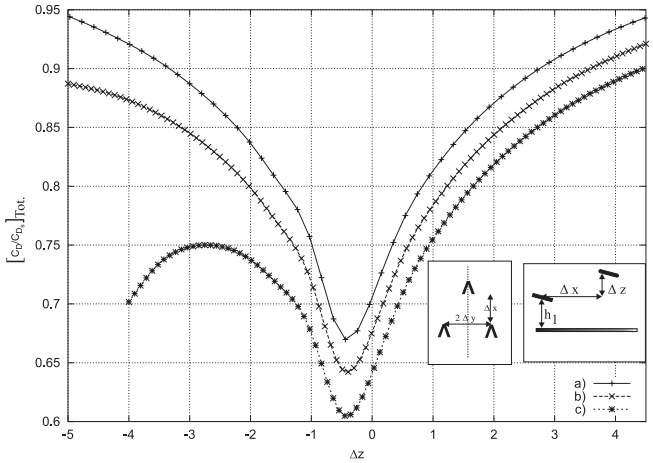

Figure 15. Total induced drag $[C_D/C_{D,s}]_{Tot}$ for a formation of three wings in ground effect *vs* Δz,
$\Delta y = 5$, $\Delta x = 3$, $\alpha_1 = 5°$.
a) $h_1 = \infty$; b) $h_1 = 10$; c) $h_1 = 5$.

https://doi.org/10.1017/S000192400000035X Published online by Cambridge University Press

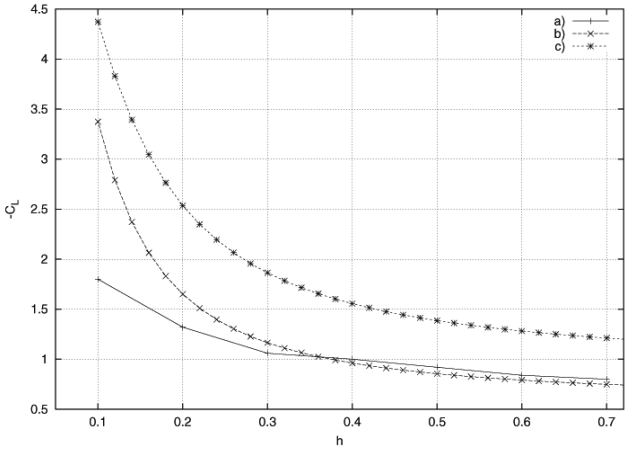

Figure 16. Lift coefficient in ground effect *vs h* at different angles-of-attack.
a) Experimental results[19], α = –1°.
b) Present calculation α = –1°, $C_{L(OGE)}$ = –0·578.
c) Present calculation = –5°, $C_{L(OGE)}$ = –0·914.

obtained by the present method are compared. In spite of the potential flow theory adopted by our approach, the trend of our results and the good comparison with the experimental data suggest that even in this very peculiar situation the method appears suitable as far as simplicity, speed and accuracy are concerned. At small distances from the ground ($h < 0{\cdot}3$), the differences between experiments and theory are due to viscosity and, above all, to turbulence in the free-stream, as reported and discussed in Ref. 23.

4.0 CONCLUSIONS

In this paper a simple model, based on the lifting line theory, has been revisited and applied to the analysis of the aerodynamic characteristics of a group of aircraft flying in formation, including the case when in the presence of ground effect. The model has been also extended to calculate the best configuration of a formation, in terms of drag reduction, by means of an optimisation algorithm and taking into account also constrained problems (such as the condition of constant lift or the conditions of pitch or roll equilibrium).

Comparisons with existing numerical and experimental data were successfully carried out and configurations corresponding to up to five aircraft were considered.

The distributions of the induced drag coefficients, both of the complete formation and of each single airplane, have been investigated as a function of the main geometrical parameters.

When the analysis was extended to take into account ground effect, a further benefit was recognised and explained in terms of the non-linear interaction between the vortex field and the ground. This last point proves to be interesting also when applications such as future developments of the aerodynamics of race cars are considered.

As a concluding remark, we note that the adopted method was shown to be an efficient tool to investigate optimal solutions when complex geometries are dealt with.

ACKNOWLEDGMENTS

This work was partially supported by the Ministry of the Universities and Scientific and Technological Research.

Appendix A

Let *u,v,w* be the three components of the velocity that a horseshoe vortex $V(x_V,y_V,z_V)$ of semiwidth *s* induces on a control point $P(x_P,y_P, z_P)$ on a surface. The

Backwash:

$$u(x,y,z)=\frac{\Gamma_{i,j}}{4\pi}F_u(\xi,\mu,\zeta,s,\varphi)$$

$$F_u(\xi,\mu,\zeta,s,\varphi)=\frac{\zeta Cos\varphi-\eta Sin\varphi}{\xi^2+(\zeta Cos\varphi-\eta Sin\varphi)^2}\cdot$$

$$\left\{\frac{Cos\varphi(\eta+sCos\varphi)+Sin\varphi(\zeta+sSin\varphi)}{\xi^2+(\eta+sCos\varphi)^2+(\zeta+sSin\varphi)^2}-\frac{Cos\varphi(\eta-sCos\varphi)+Sin\varphi(\zeta-sSin\varphi)}{\xi^2+(\eta-sCos\varphi)^2+(\zeta-sSin\varphi)^2}\right\}$$

Sidewash:

$$v(x,y,z)=\frac{\Gamma_{i,j}}{4\pi}F_v(\xi,\mu,\zeta,s,\varphi)$$

$$F_v(\xi,\mu,\zeta,s,\varphi)=\frac{\xi Sin\varphi}{\xi^2+(\zeta Cos\varphi-\eta Sin\varphi)^2}\cdot$$

$$\left\{\frac{Cos\varphi(\eta+sCos\varphi)+Sin\varphi(\zeta+sSin\varphi)}{\xi^2+(\eta+sCos\varphi)^2+(\zeta+sSin\varphi)^2}-\frac{Cos\varphi(\eta-sCos\varphi)+Sin\varphi(\zeta-sSin\varphi)}{\xi^2+(\eta-sCos\varphi)^2+(\zeta-sSin\varphi)^2}\right\}+$$

$$\frac{(\zeta-sSin\varphi)}{\xi^2+(\eta-sCos\varphi)^2+(\zeta-sSin\varphi)^2}\left\{1-\frac{\xi}{\xi^2+(\eta-sCos\varphi)^2+(\zeta-sSin\varphi)^2}\right\}-$$

$$\frac{(\zeta+sSin\varphi)}{\xi^2+(\eta+sCos\varphi)^2+(\zeta+sSin\varphi)^2}\left\{1-\frac{\xi}{\xi^2+(\eta+sCos\varphi)^2+(\zeta+sSin\varphi)^2}\right\}$$

Downwash:

$$w(x,y,z)=\frac{\Gamma_{i,j}}{4\pi}F_w(\xi,\mu,\zeta,s,\varphi)$$

$$F_w(\xi,\mu,\zeta,s,\varphi)=\frac{-\xi Cos\varphi}{\xi^2+(\zeta Cos\varphi-\eta Sin\varphi)^2}\cdot$$

$$\left\{\frac{Cos\varphi(\eta+sCos\varphi)+Sin\varphi(\zeta+sSin\varphi)}{\xi^2+(\eta+sCos\varphi)^2+(\zeta+sSin\varphi)^2}-\frac{Cos\varphi(\eta-sCos\varphi)+Sin\varphi(\zeta-sSin\varphi)}{\xi^2+(\eta-sCos\varphi)^2+(\zeta-sSin\varphi)^2}\right\}-$$

$$\frac{(\zeta-sSin\varphi)}{\xi^2+(\eta-sCos\varphi)^2+(\zeta-sSin\varphi)^2}\left\{1-\frac{\xi}{\xi^2+(\eta-sCos\varphi)^2+(\zeta-sSin\varphi)^2}\right\}+$$

$$\frac{(\zeta+sSin\varphi)}{\xi^2+(\eta+sCos\varphi)^2+(\zeta+sSin\varphi)^2}\left\{1-\frac{\xi}{\xi^2+(\eta+sCos\varphi)^2+(\zeta+sSin\varphi)^2}\right\}$$

The coordinates ξ, η, ζ of *P* are, $\xi = x_V\text{-}x_P$, $\eta = y_V\text{-}y_P$, $\zeta = z_V\text{-}z_P$ with respect to the horseshoe vortex, and is the twist angle of the surface with respect to the plane *x,y*.

In general the same equations hold for the induced velocity in any point of the aerodynamic field for = 0.

REFERENCES

1. LISSAMAN, P.B.S. and SHOLLENBERGER, C.A., Formation Flight of Birds, Science, 1970, **168**, pp 1003-1005.
2. HAINSWORTH, F. R. Precision and Dynamics of Positioning by Canada Geese Flying in Formation. *J Experimental Biology*, 1987, **128**, pp 445-462.
3. HAINSWORTH, F.R. Induced drag savings from ground effect and formation flight in brown pelicans., *J Experimental Biology*, 1988, **135**, pp 431-444.
4. HUMMEL, D. Aerodynamic aspects of formation flight in birds, *J Theoretical Biology*, 1983, **104**, (3), pp 321-347.
5. KROO, I. Drag due to lift: concepts for prediction and reduction, *Annu Rev Fluid Mech*, 2001, **33**, pp 587-617.

https://doi.org/10.1017/S000192400000035X Published online by Cambridge University Press

6. IGLESIAS, S., MASON, W.H. Optimum spanloads in formation flight, AIAA-2002-0258, 40th AIAA Aerospace Sciences Meeting & Exhibit, 14-17 January 2002 Reno, NV.
7. HOERNER, S.F. *Fluid-Dynamic Drag*, Published by the author, 1958.
8. BLOY, A.W. and TROCHALIDIS, V. The aerodynamics interference between tanker and receiver aircraft during air-to-air refueling, *Aeronaut J*, **94,** (937), 1990, pp 165-171.
9. CAMPBELL, G.S. Finite-step method for the calculation of span loadings of unusual plan forms., NACA RM L50L13, 1951.
10. BLACKWELL, J.A. A finite-step method for the calculation of theoretical load distributions for arbitrary lifting-surface arrangement at subsonic speed., NASA TN D-5335, 1969.
11. ANDERSON, J.D. *Fundamentals of Aerodynamics*, 2nd Ed, McGraw-Hill, New York, 1991.
12. KATZ, J. and PLOTKIN, A. *Low Speed Aerodynamics*, McGraw-Hill, New York, 1991.
13. RASMUSSEN, M.L. and SMITH, D.E. Lifting-line theory for arbitrary shaped wings, *J Aircr*, 1999, **36**, (2), pp 340-348.
14. WEISSINGER, J. The lift distribution of swept back wings, NACA TM 1120, 1947.
15. POWELL, M.J.D. *Numerical Methods for Constrained Optimization*, P.E. GILL & W. MURRAY (Eds), Academic Press, 1974.
16. MUNK, M.M. The minimum induced drag of airfoils, NACA Rept 121, 1921.
17. POLHAMUS, E.C. Prediction of vortex-lift characteristics by a leading-edge suction analog, *J Aircr*, 1971, **8**, (4), pp 193-199.
18. BARLETT, G.E. and VIDAL. R.J. Experimental investigation of influence of edge shape on aerodynamic characteristics of low aspect ratio wings at low speeds, *J Aero Sciences*, 1955, **22**, (8), pp 517-533.
19. RAY, R.J., COBLEIGH, B.R., VACHON, M.J. and JOHN, C.S. Flight test techniques used to evaluated performance benefits during formation flight. NASA/TP-2002-210730, August 2002.
20. ROZHDESTVENSKY, K.V. *Aerodynamics of a Lifting System in Extreme Ground Effect*, Springer, 2000.
21. BESYADOVSKIY, A.R., KORNEV, N.V. and TRESHKOV, V.K. Numerical method of calculation of aerodynamic characteristics of ekaranoplan, Proc 1st International Conference on Ekranoplans, Marine Technical University, 3 –5 May 1993,Saint-Petersburg, pp 48-65.
22. LAURENZO, R. A Long wait for big wigs, *Aerospace America*, June 2003, pp 36-40.
23. ZERINAH, J. and ZHANG, X. Aerodynamics of a single element wing in ground effect., *J Aircr*, 2000, **37**, (6), pp 1058-1064.

https://doi.org/10.1017/S000192400000035X Published online by Cambridge University Press